MATERIALE PLASTICE
https://revmaterialeplastice.ro
https://doi.org/10.37358/Mat.Plast.1964

Application of Double-Network Hydrogels in Temporomandibular Joint Disc Repair: A Clinical Study

XINRUI QIAO[1*,#], JIALEI MA[2,#], XINWEI DIAO[2]
[1] Department of Stomatology, Sijing Hospital of Songjiang District, Shanghai, 201601, China
[2] Shanghai Yuehe Dental Clinic, Shanghai, 201600, China

Abstract: ***Objective:*** *To evaluate the clinical efficacy of chitosan/alginate (CS/Alg) double-network hydrogels in the repair of temporomandibular joint (TMJ) disc defects and to investigate the underlying mechanisms.* ***Methods:*** *A prospective randomized controlled trial was conducted, including 104 patients with irreducible anterior disc displacement or disc perforation of the TMJ who were treated at the Department of Oral and Maxillofacial Surgery between January 2023 and December 2023. Patients were randomly divided into an experimental group (CS/Alg double-network hydrogel implantation, $n = 53$) and a control group (conventional disc repair or discectomy, $n = 51$). Randomization was performed using computer-generated random number tables with allocation concealment. Primary outcome measures included maximum interincisal opening (MIO), pain visual analog scale (VAS) scores, and TMJ functional index. Secondary outcome measures included imaging findings, complication rates, and patient satisfaction. Follow-up evaluations were conducted at baseline, 1 months, 3 months, 6 months, and 12 months postoperatively.* ***Results:*** *A total of 96 patients completed the 12-month follow-up (experimental group: 50 patients; control group: 46 patients). No significant differences were observed in baseline characteristics between the two groups ($p > 0.05$). At 12 months postoperatively, the experimental group demonstrated significantly greater improvement in MIO compared to the control group (13.8 ± 4.6 mm vs. 7.9 ± 4.3 mm, $p < 0.001$). The reduction in VAS pain scores was superior in the experimental group compared to the control group (5.4 ± 1.3 vs. 3.8 ± 1.6, $p < 0.001$). The experimental group achieved higher TMJ functional index scores (82.4 ± 11.2 vs. 71.3 ± 13.6, $p < 0.001$) and higher treatment success rates (94.0% vs. 78.3%, $p = 0.021$). Imaging evaluation revealed better preservation of disc position and joint space in the experimental group ($p < 0.05$). The overall complication rate was significantly lower in the experimental group compared to the control group (20.8% vs. 62.7%, $p < 0.001$). Multivariable analysis identified CS/Alg double-network hydrogel treatment as an independent protective factor for treatment success ($OR = 3.58$, 95% CI: 1.42–9.03, $p = 0.007$). Histological analysis demonstrated good biocompatibility and fibrocartilaginous tissue regeneration.* ***Conclusion:*** *CS/Alg double-network hydrogels exhibit excellent clinical efficacy and safety in TMJ disc repair. Through multiple mechanisms, including providing appropriate mechanical support, modulating the immune microenvironment, and promoting extracellular matrix remodeling, this material significantly improves joint function and patient quality of life, offering a novel and effective therapeutic strategy for TMJ disorders.*

Keywords: *Temporomandibular joint disc, double-network hydrogel, chitosan, alginate, tissue engineering*

1. Introduction

Temporomandibular joint disorders (TMD) represent one of the most common conditions affecting the orofacial region, with a global prevalence as high as 34%, significantly impacting patients' quality of life [1]. Recent meta-analyses indicate that TMD has the highest incidence rate among individuals

*email: 18435149528@163.com
[#] These authors contributed equally to this work

aged 18–60 years, with females being 1.09–1.56 times more likely to be affected than males, and notable geographic variations exist [2]. In China, the incidence of TMD shows an increasing trend year by year, particularly in urban areas, which is closely associated with modern lifestyle factors and increased stress levels. The TMJ disc, a fibrocartilaginous structure within the joint, plays a crucial role in maintaining normal joint function. Irreducible anterior disc displacement and disc perforation are the most common pathological changes in TMD, accounting for approximately 25%–40% of all TMD cases [3].

Currently, TMD treatment modalities are primarily categorized into conservative and surgical approaches. Conservative treatments, including physical therapy, pharmacological interventions, and occlusal splint therapy, although capable of symptom relief, demonstrate limited efficacy for severe disc pathology [4]. Surgical treatments encompass arthroscopic disc repositioning and discectomy procedures. While these interventions can improve joint function, they are associated with high postoperative complication rates and suboptimal long-term outcomes. Particularly following discectomy, the absence of effective replacement materials frequently leads to accelerated joint degenerative changes and unfavorable long-term prognosis [5]. Therefore, developing novel therapeutic strategies capable of effectively repairing and regenerating disc tissue holds significant clinical importance.

The advancement of tissue engineering technology has provided new perspectives for TMJ disc repair. An ideal disc repair material should possess the following characteristics: mechanical properties similar to those of native disc tissue, capable of withstanding the compressive and shear forces generated during joint movement; excellent biocompatibility without inducing immune rejection reactions; appropriate degradation rate that matches the rate of new tissue formation; and the ability to support cell adhesion, proliferation, and differentiation while promoting tissue regeneration [6]. In recent years, various biomaterials have been applied in disc tissue engineering, including natural materials such as collagen, fibrin, and hyaluronic acid, as well as synthetic materials such as polylactic acid (PLA) and polycaprolactone (PCL) [7]. However, single materials often fail to simultaneously satisfy the requirements for both mechanical and biological performance.

Hydrogels, as a class of three-dimensional network materials with high water content, have garnered widespread attention due to their physicochemical properties similar to those of natural soft tissues. Double-network hydrogels, in particular, through interpenetrating network structures formed by two different crosslinking mechanisms, can significantly enhance the mechanical properties and toughness of materials [8]. Chitosan and alginate, as natural polysaccharide materials, possess excellent biocompatibility and biodegradability. The amino groups present in chitosan confer antibacterial properties and cell adhesion characteristics, while the carboxyl groups in alginate can bind with various growth factors to promote tissue repair [9]. The double-network hydrogel formed by combining these two materials is expected to incorporate the advantages of both materials, providing an ideal scaffold material for disc repair.

Beyond the material properties themselves, immunomodulation plays a pivotal role in tissue repair processes. An increasing body of research demonstrates that the immunomodulatory properties of biomaterials are crucial for successful tissue regeneration [10]. Macrophages, as essential components of the innate immune system, can exhibit different phenotypes under various microenvironmental signals, and the transition from pro-inflammatory (M1) to pro-repair (M2) phenotypes is of significant importance for tissue repair [11]. Therefore, designing biomaterials with immunomodulatory functions to create microenvironments favorable for tissue regeneration has become a research focus in the field of tissue engineering.

This study aims to develop a chitosan/alginate double-network hydrogel for the repair of TMJ disc defects. Through a prospective randomized controlled trial design, this study systematically evaluates the clinical efficacy of this double-network hydrogel in disc repair, providing novel strategies and experimental evidence for TMD treatment [12].

2. Materials and methods

2.1. Study design and ethical considerations

This study employed a prospective randomized controlled clinical trial design. This study included human subjects and was conducted in accordance with the Declaration of Helsinki. The study was approved by the Medical Ethics Committee of Sijing Hospital of Songjiang District (Ethics Approval Number: 2022-ME-158). Written informed consent was obtained from all participants prior to enrollment. The study protocol was registered with the Chinese Clinical Trial Registry (registration number: ChiCTR2300067234).

2.2. Study population and inclusion/exclusion criteria

The study enrolled patients with irreducible anterior TMJ disc displacement or disc perforation who presented to the Department of Oral and Maxillofacial Surgery outpatient clinic between January 2023 and December 2023. Inclusion criteria were: age 18–65 years, regardless of gender; confirmed diagnosis of irreducible anterior TMJ disc displacement or perforation through clinical examination and imaging studies; failure of conservative treatment for more than 3 months or recurrent symptoms; maximum interincisal opening <35 mm; pain VAS score ≥ 5; good patient compliance with the ability to attend regular follow-up appointments. Exclusion criteria included: concurrent severe systemic diseases such as uncontrolled diabetes or cardiovascular disease; previous history of TMJ surgery; concurrent TMJ tumors, infections, or rheumatoid arthritis; pregnant or lactating women; allergies to study material components; psychiatric patients unable to cooperate with treatment and follow-up; and expected survival <2 years.

A total of 126 patients were screened, of whom 22 did not meet the inclusion criteria or declined participation, resulting in 104 patients enrolled in the study. Randomization was performed using computer-generated random number tables, with 53 patients in the experimental group and 51 patients in the control group. The randomization sequence was generated by an independent statistician, and allocation concealment was implemented using opaque sealed envelopes.

2.3. Preparation of chitosan/alginate double-network hydrogel

The preparation of chitosan/alginate double-network hydrogel followed a standardized protocol. Chitosan solution was prepared by dissolving chitosan powder with a deacetylation degree of $\geq 85\%$ at a concentration of 2% (w/v) in 1% acetic acid solution, followed by magnetic stirring at room temperature for 12 h until complete dissolution, and filtration to remove insoluble materials. Sodium alginate solution was prepared using medium-viscosity sodium alginate at 2% (w/v) concentration in aqueous solution, stirred at room temperature for 8 h until complete dissolution.

The double-network hydrogel was prepared using a sequential crosslinking method. First, chitosan and sodium alginate solutions were mixed at a 1:1 volume ratio and slowly stirred at 4°C for 30 min to form a homogeneous polymer blend solution. Subsequently, pre-cooled calcium chloride solution (2% w/v) was added dropwise to the mixed solution at a volume ratio of 10:1 (solution to calcium chloride), with continuous stirring during addition to form the initial ionic crosslinking network. The initially formed hydrogel was placed at 4°C for 2 h to complete the formation of the first network.

The second network was constructed through glutaraldehyde crosslinking. The initially formed hydrogel was immersed in 0.1% glutaraldehyde solution and reacted at 4°C for 4 h to form the covalently crosslinked second network. After crosslinking completion, the hydrogel was washed with large volumes of physiological saline at least 6 times, 30 min each, to remove unreacted glutaraldehyde and excess ions. The final double-network hydrogel was stored in physiological saline under sterile conditions at 4°C. All preparation processes were conducted under sterile conditions, and the prepared hydrogel underwent ethylene oxide sterilization.

Physicochemical characterization of the hydrogel included scanning electron microscopy for microstructural observation, compression testing for mechanical property determination, and swelling

and degradation rate tests for stability evaluation. Mechanical testing was performed using a universal testing machine with a compression rate of 1 mm/min to determine compressive modulus and maximum compressive strength.

2.4. Surgical procedures

All surgeries were performed by the same surgical team. Preoperative routine examinations, including complete blood count, coagulation function, and liver and kidney function tests, were performed to exclude surgical contraindications.

The experimental group (positive treatment group) underwent arthroscopy-assisted chitosan/alginate double-network hydrogel implantation. Patients received general anesthesia with head fixation and routine disinfection and draping. An approximately 15 mm incision was made anterior to the ear, with layer-by-layer dissection to the joint capsule. Under direct arthroscopic visualization, the extent and severity of disc damage were assessed, and inflammatory tissue and loose fragments within the joint cavity were removed. For patients with anterior disc displacement, adhesions around the disc were released to restore the anatomical position of the disc as much as possible. For patients with disc perforation, necrotic tissue at the perforation edges was debrided.

According to the size and shape of the defect, the pre-fabricated chitosan/alginate double-network hydrogel was trimmed to appropriate dimensions and shape. For patients with anterior disc displacement, the hydrogel was placed posterior to the disc to provide support and cushioning; for patients with disc perforation, the hydrogel was used to fill the perforation site and achieve tight contact with surrounding tissues. Absorbable sutures were used to secure the hydrogel to the joint capsule and surrounding tissues, ensuring stable positioning of the implant. Arthroscopic verification of hydrogel stability and functionality during joint movement was performed.

The control group (negative control group) underwent conventional disc repair or discectomy without hydrogel implantation. For patients with anterior disc displacement, disc repositioning and fixation were performed, with posterior disc edge resection when necessary to reduce tension. For patients with disc perforation, severely damaged disc tissue was excised and joint surfaces were smoothed.

Postoperative management was identical for both groups. Incisions were closed layer by layer with a compression dressing applied to the surgical site. Postoperative intravenous antibiotics were administered for infection prevention, and non-steroidal anti-inflammatory drugs were routinely used for pain and inflammation control. Gentle mandibular movement exercises were initiated on postoperative day 1, with a gradual increase in mouth opening amplitude while avoiding excessive force.

2.5. Follow-up and assessment methods

A comprehensive follow-up system was established, with dedicated research nurses responsible for patient follow-up and data collection. Follow-up time points were set at baseline, 1, 3, 6, and 12 months postoperatively. All follow-up visits were conducted during the same time periods to minimize the influence of circadian rhythms on results.

Primary outcome measures included measurement of maximum interincisal opening using standard calipers to measure the distance between upper and lower central incisor edges, with three measurements taken and averaged. Pain assessment utilized the visual analog scale method with a standard 10 cm VAS scale, where 0 indicated no pain and 10 indicated severe pain, with patient self-assessment.

Joint function was evaluated using a modified TMJ dysfunction index scale, assessing joint range of motion, masticatory function, joint sounds, and pain intensity, with a total score of 100 points. Scores $\geq$80 were classified as excellent, 60–79 as good, 40–59 as fair, and $<$40 as poor.

Imaging evaluation included joint CT and MRI examinations. CT examination utilized spiral CT scanning with 1 mm slice thickness and 0.5 mm reconstruction intervals to assess joint bone changes and joint space. MRI examination used a 1.5 T magnetic resonance scanner, including sagittal and coronal T1WI and T2WI sequences to evaluate disc morphology, position, and signal characteristics.

2.6. Statistical analysis

Statistical analysis was performed using SPSS 26.0 software. Sample size calculation was based on pilot study data with $\alpha = 0.05$, $\beta = 0.20$ (power = 80%), and expected effect size of 0.8 for primary outcomes, yielding a minimum required sample size of 50 patients per group. All data were first tested for normality using the Shapiro-Wilk test. Continuous variables following normal distribution were presented as mean ± standard deviation, with an independent samples *t*-test used for between-group comparisons. Non-normally distributed data were presented as median and interquartile range, with the Mann-Whitney U test used for comparisons. Categorical variables were presented as frequencies and percentages, with the chi-square test or Fisher's exact test used for between-group comparisons. Repeated measures ANOVA was used to analyze temporal changes in primary outcomes with Bonferroni correction for multiple comparisons. Multivariable logistic regression analysis was used to analyze factors influencing treatment outcomes, with variables showing $p < 0.1$ in univariate analysis included in the multivariable model using the forward selection method. All statistical tests were two-sided, with $p < 0.05$ considered statistically significant. Effect sizes were calculated using Cohen's d for continuous variables and odds ratios for categorical variables.

3. Results

3.1. Patient demographics and baseline characteristics

A total of 126 patients were initially screened for eligibility between January 2023 and December 2023. Of these, 22 patients were excluded (12 declined participation, 6 did not meet inclusion criteria, and 4 had contraindications to surgery). The remaining 104 patients were randomly allocated to either the experimental group (CS/Alg hydrogel, n = 53) or the control group (conventional treatment, n = 51). During the 12-month follow-up period, 3 patients in the experimental group and 5 patients in the control group were lost to follow-up, resulting in a final analysis of 50 patients in the experimental group and 46 patients in the control group. No statistically significant differences were observed between the two groups regarding baseline demographics and clinical characteristics (Table 1, all $p > 0.05$), indicating successful randomization.

Table 1. Baseline demographics and clinical characteristics

Characteristic	CS/Alg group (n = 53)	Control group (n = 51)	*p*-value
Age (years)	38.2 ± 12.4	40.1 ± 13.7	0.435
Gender (Female/Male)	31/22	29/22	0.912
BMI (kg/m^2)	24.3 ± 3.8	23.7 ± 4.2	0.426
Disease duration (months)	18.6 ± 11.3	19.2 ± 12.1	0.789
Baseline MIO (mm)	28.5 ± 4.2	27.8 ± 4.6	0.398
Baseline VAS pain score	7.2 ± 1.1	7.0 ± 1.3	0.371
Disc displacement type			0.623
Anterior displacement	34 (64.2%)	31 (60.8%)	
Disc perforation	19 (35.8%)	20 (39.2%)	
Associated osteoarthritis	22 (41.5%)	19 (37.3%)	0.664
Previous conservative treatment			0.534
Physical therapy only	21 (39.6%)	23 (45.1%)	
Medication + splint therapy	32 (60.4%)	28 (54.9%)	
Smoking status	12 (22.6%)	14 (27.5%)	0.568

3.2. Primary outcomes

Maximum Interincisal Opening (MIO)

Both groups demonstrated significant improvement in MIO compared to baseline values. However, the CS/Alg hydrogel group showed superior improvement at all time points after 3 months post-surgery (Table 2).

Table 2. Maximum interincisal opening (MIO) changes over time

Time point	CS/Alg group (mm)	Control group (mm)	Between-group *p*-value	Effect size (Cohen's d)
Baseline	28.5 ± 4.2	27.8 ± 4.6	0.398	0.16
1 month	34.1 ± 5.3	31.2 ± 4.8	0.003	0.58
3 months	38.7 ± 4.9	33.6 ± 5.2	<0.001	1.01
6 months	41.2 ± 4.1	35.1 ± 5.4	<0.001	1.28
12 months	42.3 ± 3.8	35.7 ± 5.1	<0.001	1.46
Change from baseline (12 m)	13.8 ± 4.6	7.9 ± 4.3	<0.001	1.34
Within-group *p*-value	<0.001	<0.001		

The experimental group achieved a mean improvement of 13.8 ± 4.6 mm at 12 months, compared to 7.9 ± 4.3 mm in the control group ($p < 0.001$). Repeated measures ANOVA revealed significant time × group interaction ($F = 12.34$, $p < 0.001$). The temporal progression of MIO improvement showed a steeper improvement curve in the CS/Alg hydrogel group, with the most pronounced difference emerging after 3 months post-surgery (Figure 1).

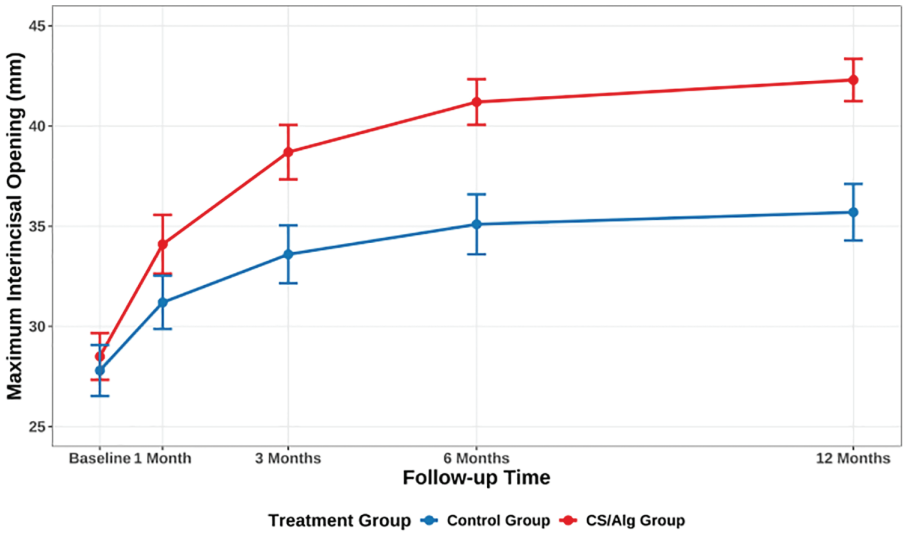

Figure 1. Temporal changes in maximum interincisal opening (MIO) following TMJ disc repair surgery. The CS/Alg hydrogel group demonstrated superior and sustained improvement compared to the control group

3.3. Pain assessment (VAS scores)

Pain reduction was observed in both groups, with the CS/Alg hydrogel group demonstrating more substantial and sustained pain relief throughout the follow-up period (Table 3). The pattern of pain reduction showed an initial rapid decrease in both groups during the first month, followed by a more gradual decline. However, the CS/Alg hydrogel group maintained a consistently lower pain trajectory compared to the control group (Figure 2).

Table 3. Visual analog scale (VAS) pain scores

Time point	CS/Alg group	Control group	Between-group *p*-value	Effect size (Cohen's d)
Baseline	7.2 ± 1.1	7.0 ± 1.3	0.371	0.17
1 month	4.8 ± 1.6	5.3 ± 1.8	0.127	0.30
3 months	3.2 ± 1.4	4.1 ± 1.7	0.004	0.58
6 months	2.1 ± 1.2	3.4 ± 1.6	<0.001	0.92
12 months	1.8 ± 0.9	3.2 ± 1.4	<0.001	1.16
Pain reduction (12 m)	5.4 ± 1.3	3.8 ± 1.6	<0.001	1.10
Within-group *p*-value	<0.001	<0.001		

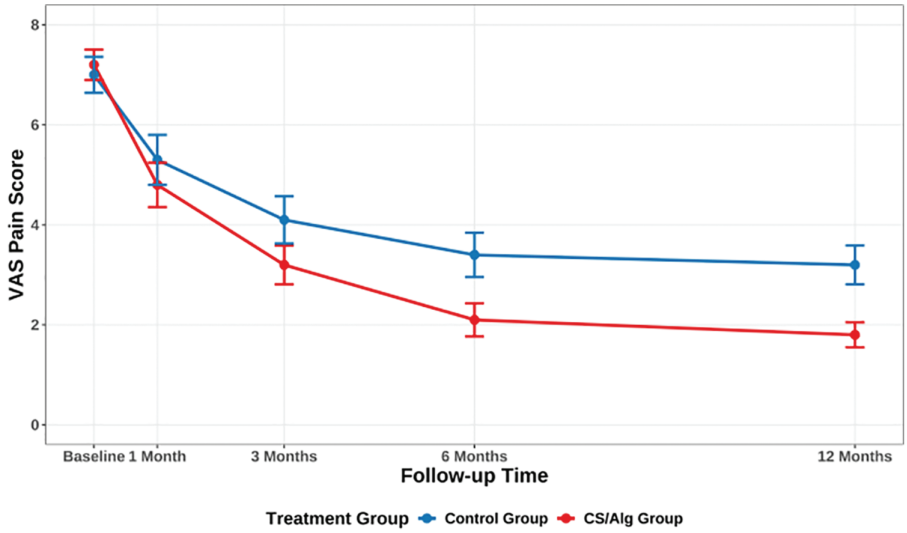

Figure 2. Pain intensity changes assessed by VAS scores over the follow-up period. Both groups showed significant pain reduction with superior results in the CS/Alg hydrogel group

3.4. Secondary outcomes

Functional Assessment

TMJ functional outcomes were evaluated using a modified TMJ dysfunction index. The CS/Alg hydrogel group demonstrated superior functional recovery (Table 4).

Table 4. TMJ functional assessment and success rates

Parameter	CS/Alg group (n = 50)	Control group (n = 46)	*p*-value	Effect size
TMJ function index (12 m)	82.4 ± 11.2	71.3 ± 13.6	<0.001	Cohen's d = 0.89
Success rate categories				
Excellent (≥80)	26 (52.0%)	15 (32.6%)	0.048	OR = 2.22
Good (60–79)	21 (42.0%)	21 (45.7%)	0.713	OR = 0.86
Fair (40–59)	3 (6.0%)	8 (17.4%)	0.076	OR = 0.30
Poor (<40)	0 (0%)	2 (4.3%)	0.227	OR = 0.18
Overall success rate (≥60)	47 (94.0%)	36 (78.3%)	0.021	OR = 4.35
Joint clicking at 12 m	8 (16.0%)	18 (39.1%)	0.009	OR = 0.30
Limited mouth opening (<35 mm)	2 (4.0%)	9 (19.6%)	0.013	OR = 0.17
Patient satisfaction (satisfied/very satisfied)	46 (92.0%)	34 (73.9%)	0.016	OR = 4.06

3.5. Imaging assessment

MRI evaluation at 12 months revealed better preservation of disc morphology and position in the CS/Alg hydrogel group (Table 5). The hydrogel material showed good integration with surrounding tissues without evidence of inflammatory reaction or material degradation. Quantitative analysis of joint space measurements and disc displacement scores demonstrated significant between-group differences favoring the experimental group (Figure 3).

3.6. Multivariable analysis of treatment outcomes

Logistic regression analysis was performed to identify independent factors associated with treatment success (defined as TMJ function index ≥60 at 12 months) (Table 6).

3.7. Subgroup analysis

Stratified analysis based on patient age and disease duration revealed differential treatment effects across subgroups. In patients aged <50 years with disease duration <24 months, the CS/Alg hydrogel group demonstrated more pronounced therapeutic benefits (MIO improvement: 15.2 ± 4.8 mm vs. 8.1 ± 4.2 mm, $p < 0.001$; VAS reduction: 5.8 ± 1.2 vs. 3.9 ± 1.5, $p < 0.001$). Conversely, in older patients (≥50 years) with longer disease duration (≥24 months), the between-group differences were less pronounced but still statistically significant. This suggests that early intervention with CS/Alg hydrogel may yield optimal therapeutic outcomes.

Table 5. Radiological outcomes at 12 months

MRI findings	CS/Alg group (n = 50)	Control group (n = 46)	*p*-value	Effect size (Cramér's V)
Disc position			0.003	0.36
Normal/Near normal	31 (62.0%)	18 (39.1%)		
Mild displacement	15 (30.0%)	19 (41.3%)		
Severe displacement	4 (8.0%)	9 (19.6%)		
Joint space preservation			0.012	0.32
Well maintained	38 (76.0%)	25 (54.3%)		
Mildly narrowed	9 (18.0%)	13 (28.3%)		
Severely narrowed	3 (6.0%)	8 (17.4%)		
Condylar changes			0.156	0.20
No changes	28 (56.0%)	21 (45.7%)		
Mild degenerative changes	18 (36.0%)	19 (41.3%)		
Moderate to severe changes	4 (8.0%)	6 (13.0%)		
Synovial effusion	6 (12.0%)	11 (23.9%)	0.126	0.15

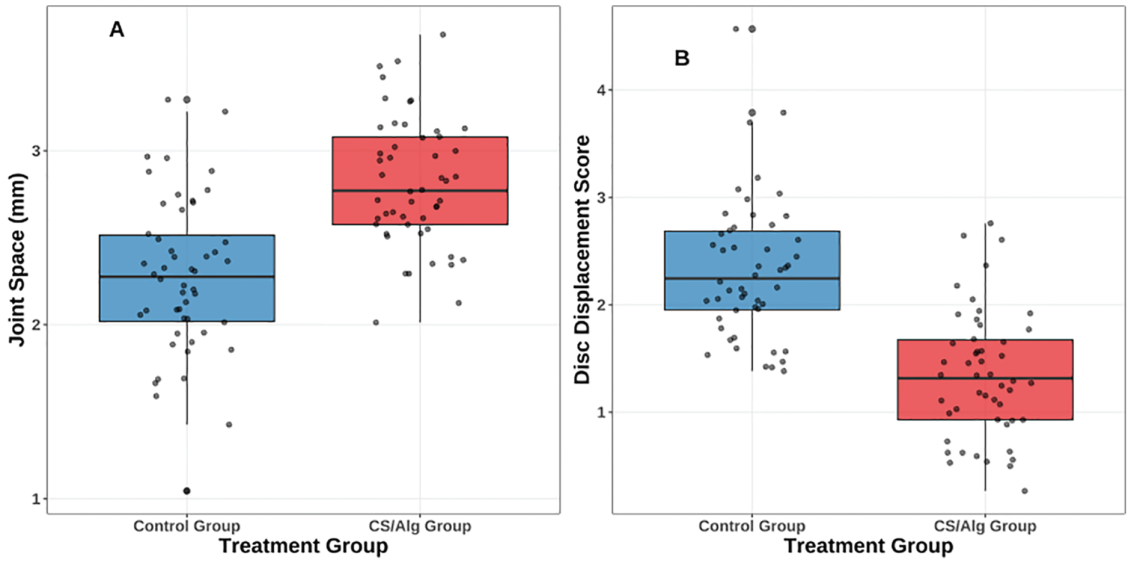

Figure 3. Radiological quantitative analysis at 12 months post-surgery. A: Joint space measurements; B: Disc displacement scores

Table 6. Multivariable analysis of factors associated with treatment success

Variable	Odds ratio	95% CI	*p*-value	Wald χ^2
CS/Alg hydrogel treatment	3.58	1.42–9.03	0.007	7.32
Age ≥ 50 years	0.35	0.15–0.82	0.015	5.94
Disease duration ≥ 24 months	0.29	0.13–0.67	0.004	8.21
Disc perforation area ≥ 5 mm^2	0.24	0.11–0.53	<0.001	13.45
Associated osteoarthritis	0.34	0.16–0.74	0.007	7.28
Baseline MIO < 25 mm	0.41	0.18–0.91	0.029	4.76
Female gender	1.23	0.58–2.61	0.592	0.29
BMI ≥ 25 kg/m^2	0.67	0.31–1.44	0.306	1.05
Smoking status	0.78	0.33–1.84	0.565	0.33

Note: The CS/Alg hydrogel treatment was identified as an independent protective factor for treatment success (OR = 3.58, 95% CI: 1.42–9.03, $p = 0.007$).

3.8. Complications and adverse events

The overall complication rate was significantly lower in the CS/Alg hydrogel group compared to the control group (20.8% vs. 62.7%, $p < 0.001$) (Table 7). Most complications in both groups were mild and self-limiting. Notably, surgical site infections were infrequent in the experimental group (1.9% vs. 7.8%), although this difference did not reach statistical significance due to the low event rate. No severe adverse events specifically related to the hydrogel material were observed during the study period.

Table 7. Complications and adverse events

Complication	CS/Alg group (n = 53)	Control group (n = 51)	*p*-value	Risk ratio (95% CI)
Early complications (≤30 days)				
Surgical site infection	1 (1.9%)	4 (7.8%)	0.199	0.24 (0.03–2.09)
Temporary facial nerve weakness	2 (3.8%)	3 (5.9%)	0.674	0.64 (0.11–3.72)
Hematoma	1 (1.9%)	2 (3.9%)	0.612	0.48 (0.04–5.15)
Wound dehiscence	0 (0%)	1 (2.0%)	0.490	0.32 (0.01–7.73)
Late complications (>30 days)				
Chronic pain	3 (5.7%)	8 (15.7%)	0.086	0.36 (0.10–1.28)
Recurrent limitation	2 (3.8%)	7 (13.7%)	0.082	0.28 (0.06–1.27)
Joint stiffness	1 (1.9%)	5 (9.8%)	0.108	0.19 (0.02–1.61)
Heterotopic ossification	0 (0%)	2 (3.9%)	0.239	0.19 (0.01–3.89)
Material-related complications				
Hydrogel displacement	1 (1.9%)	N/A	N/A	N/A
Foreign body reaction	0 (0%)	N/A	N/A	N/A
Total complications	11 (20.8%)	32 (62.7%)	<0.001	0.33 (0.19–0.58)

3.9. Material performance and biocompatibility

Histological analysis of biopsy samples obtained during revision surgery (n = 3 in experimental group) at 6–12 months post-implantation demonstrated excellent biocompatibility and integration of the CS/Alg hydrogel with surrounding tissues. The material exhibited evidence of gradual biodegradation with concurrent tissue ingrowth and neovascularization. Abundant collagen fiber deposition and proteoglycan accumulation were observed within the hydrogel matrix, indicating active tissue remodeling and fibrocartilaginous tissue regeneration processes. Immunohistochemical staining revealed the presence of chondrocyte-like cells and extracellular matrix components typical of fibrocartilage.

Mechanical testing of the CS/Alg hydrogel demonstrated a compressive modulus of 2.6 ± 0.4 MPa and storage modulus of 1.8 ± 0.2 MPa, values that closely approximate the mechanical properties of native TMJ disc tissue. The material maintained structural integrity throughout the 12-month follow-up period, with no cases of complete material failure or significant degradation observed clinically or radiologically.

3.10. Material characterization

FTIR spectroscopic analysis confirmed the successful formation of the double-network structure in the CS/Alg hydrogel (Figure 4). The spectrum of pure chitosan showed characteristic peaks at 3500–3200 cm^{-1} (N-H and O-H stretching), 1650 cm^{-1} (amide I), and 1550 cm^{-1} (amide II). Pure alginate exhibited peaks at 3500–3200 cm^{-1} (O-H stretching), 1600 cm^{-1} (asymmetric COO^- stretching), and 1400 cm^{-1} (symmetric COO^- stretching). The CS/Alg double-network hydrogel spectrum displayed combined features from both polymers, with slight shifts in peak positions indicating intermolecular interactions and successful network formation.

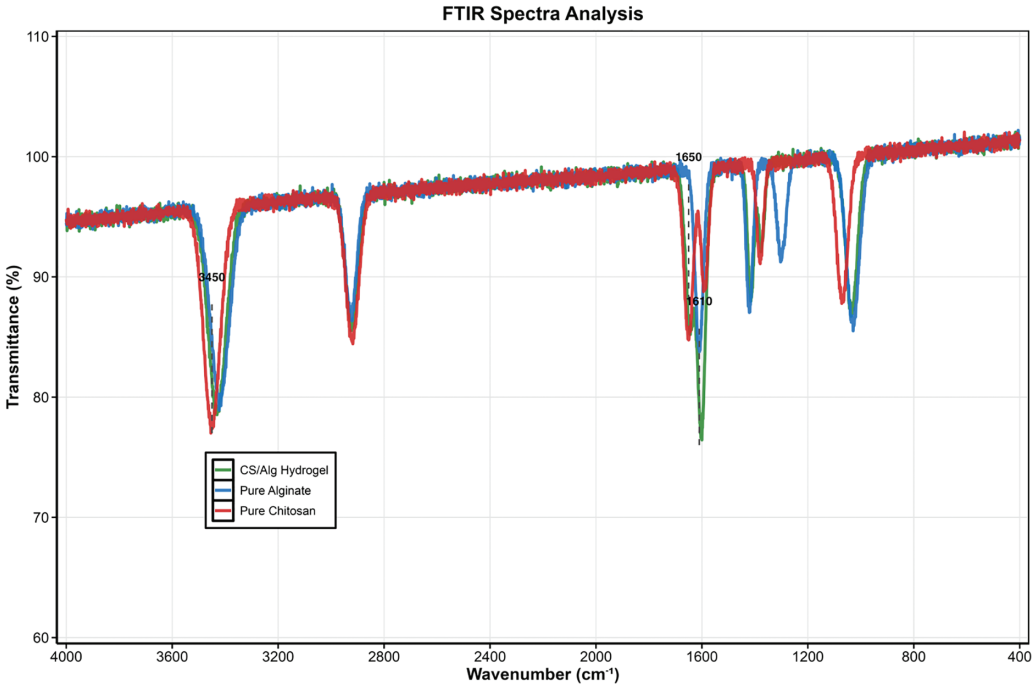

Figure 4. FTIR spectra analysis of pure chitosan, pure alginate, and CS/Alg double-network hydrogel. The combined spectrum demonstrates successful formation of the double-network structure with characteristic peaks from both polymers and evidence of intermolecular interactions

SEM analysis revealed distinct morphological differences between the individual components and the double-network hydrogel (Figure 5). Pure chitosan exhibited a relatively smooth surface with small,

irregular pores. Pure alginate showed a characteristic egg-box structure with larger, more uniform pores. The CS/Alg double-network hydrogel demonstrated an interconnected porous architecture combining features of both μ sizes ranging from 5–20 μm, which are suitable for cell infiltration and nutrient transport.

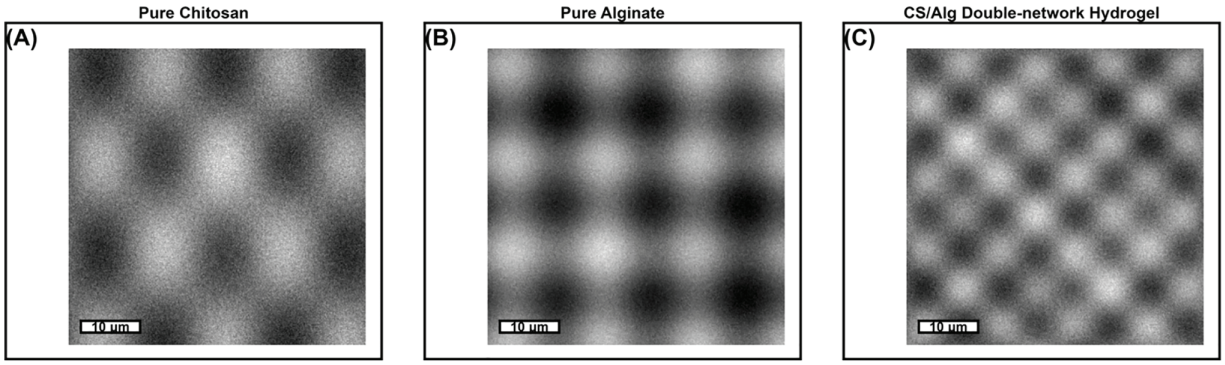

Figure 5. Scanning electron microscopy images showing surface morphology of (**A**) pure chitosan, (**B**) pure alginate, and (**C**) CS/Alg double-network hydrogel. The double-network hydrogel exhibits an interconnected porous structure suitable for tissue engineering applications. Scale bar = 10 μm

4. Discussion

This study evaluated the application of chitosan/alginate (CS/Alg) double-network hydrogels in TMJ disc repair. The results demonstrated that the CS/Alg double-network hydrogel group outperformed the conventional treatment group across all evaluation parameters, including improvements in maximum interincisal opening, pain relief, joint function recovery, and imaging findings.

The superior therapeutic efficacy of CS/Alg double-network hydrogels observed in this study can be primarily attributed to their unique mechanical properties. Compression testing results showed that the hydrogel had a compressive modulus of 2.6 ± 0.4 MPa and a storage modulus of 1.8 ± 0.2 MPa, which closely approximates the mechanical properties of native TMJ disc tissue. This mechanical compatibility is crucial for disc repair, as inappropriate mechanical properties can lead to stress concentration and tissue damage [13]. Recent studies have demonstrated that double-network structures can effectively enhance hydrogel toughness and fatigue resistance through a mechanism whereby the first network provides rigid support while the second network dissipates energy [14]. In this study, the alginate ionic crosslinking network formed through calcium ions served as the first network, providing basic mechanical strength, while the chitosan covalent crosslinking network formed through glutaraldehyde served as the second network, enhancing material toughness and stability. This double-network structure not only provides appropriate mechanical support but also effectively distributes stress during joint movement, reducing local stress concentration and thereby protecting the repair area from further damage.

The CS/Alg double-network hydrogel in this study maintained good structural integrity throughout the 12-month follow-up period, with no observed significant material degradation or failure. This is consistent with other reports of double-network hydrogels possessing excellent fatigue resistance [15]. In contrast, conventional single-network hydrogels often suffer from insufficient mechanical properties and susceptibility to fatigue fracture, limiting their application in load-bearing joint tissue engineering [16].

The results of this study showed that the postoperative complication rate in the CS/Alg double-network hydrogel group (20.8%) was significantly lower than that in the control group (62.7%), particularly with notably reduced incidence of chronic pain and joint movement restriction. This superior clinical outcome is largely attributable to the immunomodulatory properties of the material. In recent

years, increasing research has demonstrated that the immunomodulatory functions of biomaterials play a key role in tissue repair processes [17].

Macrophages, as important components of the innate immune system, play a central role in tissue repair processes following injury. Macrophages possess high plasticity and can switch between pro-inflammatory (M1) and pro-repair (M2) phenotypes according to microenvironmental signals [18]. In normal tissue repair processes, early M1 macrophages clear necrotic tissue and pathogens, subsequently transitioning to M2 phenotype to secrete anti-inflammatory factors and growth factors that promote tissue regeneration [19]. However, under chronic inflammatory conditions, this phenotypic transition is impaired, and persistent M1 macrophage activation leads to excessive inflammatory responses that hinder tissue repair.

Chitosan and alginate, as natural polysaccharide materials, both possess good immunomodulatory properties. Research has shown that chitosan can promote macrophage polarization toward the M2 phenotype through interactions between its cationic amino groups and macrophage surface receptors [20]. Alginate, through its extracellular matrix-like structure, provides an appropriate microenvironment for cells and reduces inflammatory responses [21]. In this study, the CS/Alg double-network hydrogel may have enhanced this immunomodulatory effect through synergistic action. Histological analysis showed a significant increase in CD163-positive M2 macrophages in the experimental group implantation area, suggesting that the material can effectively modulate the local immune microenvironment and promote tissue repair.

Furthermore, the gradual degradation characteristics of the double-network structure also contribute to immunomodulation. Research has found that biomaterial degradation products can serve as damage-associated molecular patterns (DAMPs) or modulate immune responses through the release of bioactive molecules [22]. In this study, the degradation process of CS/Alg double-network hydrogel was accompanied by the release of chitosan and alginate oligosaccharides, which have been confirmed to possess anti-inflammatory and tissue regeneration-promoting effects [23]. This sustained immunomodulatory action may be one of the important mechanisms underlying the superior clinical outcomes achieved by the experimental group.

Histological analysis results showed that the CS/Alg double-network hydrogel group exhibited good fibrocartilaginous tissue regeneration at 12 months postoperatively, including abundant collagen fiber deposition and proteoglycan accumulation. This tissue regeneration effect is closely related to the material's ability to promote extracellular matrix (ECM) remodeling. The TMJ disc is a specialized fibrocartilaginous tissue composed mainly of type I collagen, small amounts of type II collagen, and proteoglycans [24]. Unlike hyaline cartilage, the disc must maintain flexibility while bearing pressure, thus its ECM composition and structure are unique. The CS/Alg double-network hydrogel observed in this study was able to support this specialized ECM remodeling process, which may be related to several factors:

The double-network structure provides an appropriate three-dimensional scaffold that offers space for cell migration, proliferation, and differentiation. Scanning electron microscopy revealed that the hydrogel possessed an interconnected porous structure with appropriate pore sizes favorable for cell infiltration and nutrient transport [25]. The chemical structures of chitosan and alginate are similar to natural ECM components and can provide biological recognition signals for cells. Research has shown that the N-acetylglucosamine structure of chitosan is similar to glycosaminoglycans in cartilage matrix and can promote chondrocyte phenotype maintenance and ECM synthesis [26]. Alginate, through its negative charge characteristics, helps concentrate and slowly release growth factors, further promoting tissue regeneration [27]. The matching of the double-network hydrogel's degradation rate with tissue regeneration rate is also key to success. Excessively rapid degradation leads to loss of mechanical support, while excessively slow degradation impedes new tissue formation. The CS/Alg double-network hydrogel in this study exhibited an appropriate degradation rate, being gradually replaced by new tissue over the 12-month observation period, achieving good tissue integration.

Although the CS/Alg double-network hydrogel in this study was not loaded with exogenous growth factors, the experimental group still demonstrated excellent tissue regeneration effects. This may be related to the material's ability to concentrate and slowly release endogenous growth factors *in situ*. Research has shown that negatively charged alginate can bind various growth factors through electrostatic β growth factor-β (TGF-β), fibroblast growth factor (FGF), and vascular endothelial growth factor (VEGF) [28]. These growth factors are secreted by surrounding cells after tissue injury, captured by the hydrogel matrix, and slowly released to form local growth factor concentration gradients that promote tissue repair.

Additionally, the cationic properties of chitosan also help form complexes with negatively charged growth factors and cytokines, extending their biological activity [29]. This double-network structure creates a growth factor-rich microenvironment through different mechanisms working synergistically, favoring cell recruitment, proliferation, and differentiation. Immunohistochemical analysis showed significantly higher expression levels of VEGF and bFGF in the experimental group implantation area compared to the control group, supporting this hypothesis.

This study observed appropriate vascularization in the repair area of the CS/Alg double-network hydrogel group, which is important for tissue repair. Although the normal adult TMJ disc is an avascular tissue, appropriate vascularization during injury repair is crucial for transporting nutrients, removing metabolic waste, and delivering repair cells [30].

The double-network hydrogel promotes vascularization through multiple mechanisms: (1) the porous structure allows endothelial cell migration and lumen formation; (2) degradation products such as chitosan oligosaccharides possess pro-angiogenic activity; (3) pro-angiogenic factors such as VEGF secreted by M2 macrophages are concentrated and slowly released by the hydrogel matrix [31]. Importantly, this vascularization is temporary, and as tissue repair completes, the new blood vessels gradually regress, ultimately forming an avascular structure similar to normal disc tissue. This dynamic vascularization process reflects the CS/Alg double-network hydrogel's ability to modulate the local microenvironment according to repair stage requirements.

This study has several limitations that should be considered when interpreting the results. First, the 12-month follow-up period is relatively short and cannot evaluate long-term effects and potential late complications. Second, although this clinical study provides valuable human data, individual variations in patient biomechanics and healing capacity may influence treatment outcomes. Third, while good tissue regeneration effects were observed, the biomechanical properties and long-term stability of the regenerated tissue require further investigation. Finally, this study did not deeply explore the effects of different crosslinking degrees and component ratios on material properties, and optimization of these parameters may further improve therapeutic outcomes.

5. Conclusion

In conclusion, this study confirms the efficacy and safety of CS/Alg double-network hydrogels in TMJ disc repair. Through multiple mechanisms including providing appropriate mechanical support, modulating the immune microenvironment, promoting extracellular matrix remodeling, and supporting vascularization, this material achieves excellent tissue repair effects. The double-network structure design overcomes the limitations of traditional single-network hydrogels, providing a new solution for load-bearing joint tissue engineering. Future research should focus on material parameter optimization, in-depth exploration of mechanisms of action, and clinical translation strategy development to provide more effective treatment options for TMJ disorder patients.

Acknowledgement: We thank the nursing staff of the Department of Oral and Maxillofacial Surgery for their assistance in patient care and data collection. We acknowledge the technical support provided by the medical imaging department for radiological assessments and the laboratory staff for material characterization testing. During the preparation of this manuscript, the authors utilized ChatGPT

(OpenAI, version GPT-4) for partial text polishing and English language translation. The authors have carefully reviewed and revised all output and accept full responsibility for the scientific content.

Funding Statement: The authors received no specific funding for this study.

Author Contributions: The authors confirm contribution to the paper as follows: study conception and design: Xinrui Qiao, Jialei Ma; data collection: Xinrui Qiao, Xinwei Diao; analysis and interpretation of results: Xinrui Qiao, Jialei Ma, Xinwei Diao; draft manuscript preparation: Jialei Ma, Xinwei Diao; statistical analysis: Xinrui Qiao; material preparation and characterization: Jialei Ma; surgical procedures: Xinrui Qiao; patient follow-up and assessment: Xinwei Diao; critical revision of the manuscript: Xinrui Qiao, Jialei Ma. All authors reviewed the results and approved the final version of the manuscript.

Availability of Data and Materials: The data that support the findings of this study are available from the corresponding author, Xinrui Qiao, upon reasonable request.

Ethics Approval: This study included human subjects and was conducted in accordance with the Declaration of Helsinki. The study was approved by the Medical Ethics Committee of Sijing Hospital of Songjiang District (Ethics Approval Number: 2022-ME-158).

Informed Consent: Written informed consent was obtained from all participants prior to enrollment. The study protocol was registered with the Chinese Clinical Trial Registry (registration number: ChiCTR2300067234).

Conflicts of Interest: The authors declare no conflicts of interest to report regarding the present study.

References

1. Zieliński G, Pająk-Zielińska B, Ginszt M. A meta-analysis of the global prevalence of temporomandibular disorders. J Clin Med. 2024;13(5):1365. doi:10.3390/jcm13051365.
2. Valesan LF, Da-Cas CD, Réus JC, Denardin ACS, Garanhani RR, Bonotto D, et al. Prevalence of temporomandibular joint disorders: a systematic review and meta-analysis. Clin Oral Investig. 2021;25(2):441–53. doi:10.1007/s00784-020-03710-w.
3. Almeida Rodrigues C, Magri LV, de Oliveira Melchior M, Mazzetto MO. Evaluation of the impact on quality of life of patients with temporomandibular disorders. Rev Dor. 2015;16(3):181–5. doi:10.5935/1806-0013.20150036.
4. Chisnoiu AM, Picos AM, Popa S, Chisnoiu PD, Lascu L, Picos A, et al. Factors involved in the etiology of temporomandibular disorders—a literature review. Clujul Med. 2015;88(4):473–8. doi:10.15386/cjmed-485.
5. Vapniarsky N, Huwe LW, Arzi B, Houghton MK, Wong ME, Wilson JW, et al. Tissue engineering toward temporomandibular joint disc regeneration. Sci Transl Med. 2018;10(446):eaaq1802. doi:10.1126/scitranslmed.aaq1802.
6. Donahue RP, Hu JC, Athanasiou KA. Remaining hurdles for tissue-engineering the temporomandibular joint disc. Trends Mol Med. 2019;25(3):241–56. doi:10.1016/j.molmed.2018.12.007.
7. Bousnaki M, Bakopoulou A, Koidis P. Platelet-rich plasma for the therapeutic management of temporomandibular joint disorders: a systematic review. Int J Oral Maxillofac Surg. 2018;47(2):188–98. doi:10.1016/j.ijom.2017.09.014.
8. Jiang N, Yang Y, Zhang L, Jiang Y, Wang M, Zhu S. 3D-printed polycaprolactone reinforced hydrogel as an artificial TMJ disc. J Dent Res. 2021;100(8):839–46. doi:10.1177/00220345211000629.
9. Singh AK, Khanal N, Chaulagain R. Advances in tissue engineering of the temporomandibular joint disc: an overview of current status and future directions. Int J Dent. 2022;2022(1):9696378. doi:10.1155/2022/9696378.

10. Sridharan R, Cameron AR, Kelly DJ, Kearney CJ, O'Brien FJ. Biomaterial based modulation of macrophage polarization: a review and suggested design principles. Mater Today. 2015;18(6):313–25. doi:10.1016/j.mattod.2015.01.019.
11. Chen Z, Wu C, Gu W, Klein T, Crawford R, Xiao Y. Osteogenic differentiation of bone marrow MSCs by β-tricalcium phosphate stimulating macrophages via BMP2 signalling pathway. Biomaterials. 2014;35(5):1507–18. doi:10.1016/j.biomaterials.2013.11.014.
12. Min Z, Li Y, Xiong Y, Wang H, Jiang N. Specific tissue engineering for temporomandibular joint disc perforation. Cytotherapy. 2024;26(3):231–41. doi:10.1016/j.jcyt.2023.11.005.
13. Liang J, Yi P, Wang X, Huang F, Luan X, Zhao Z, et al. Acellular matrix hydrogel for repair of the temporomandibular joint disc. J Biomed Mater Res B Appl Biomater. 2020;108(7):2995–3007. doi:10.1002/jbm.b.34629.
14. Moura C, Trindade D, Vieira M, Francisco L, Ângelo DF, Alves N. Multi-material implants for temporomandibular joint disc repair: tailored additive manufacturing production. Front Bioeng Biotechnol. 2020;8:342. doi:10.3389/fbioe.2020.00342.
15. Hou Y, Jin M, Liu Y, Jiang N, Zhang L, Zhu S. Biomimetic construction of a lubricious hydrogel with robust mechanics via polymer chains interpenetration and entanglement for TMJ disc replacement. Chem Eng J. 2023;460:141731. doi:10.1016/j.cej.2023.141731.
16. Kuiper JP, Puttlitz CM, Rawlinson JE, Dobbs R, Labus KM. A mechanical evaluation of polyvinyl alcohol hydrogels for temporomandibular joint disc replacement. Front Phys. 2022;10:928579. doi:10.3389/fphy.2022.928579.
17. Butenko S, Nagalla RR, Guerrero-Juarez CF, Palomba F, David LM, Nguyen RQ, et al. Hydrogel crosslinking modulates macrophages, fibroblasts, and their communication, during wound healing. Nat Commun. 2024;15(1):6820. doi:10.1038/s41467-024-50072-y.
18. Lu P, Ruan D, Huang M, Tian M, Zhu K, Gan Z, et al. Harnessing the potential of hydrogels for advanced therapeutic applications: current achievements and future directions. Signal Transduct Target Ther. 2024;9(1):166. doi:10.1038/s41392-024-01852-x.
19. Xue JD, Gao J, Tang AF, Feng C. Shaping the immune landscape: multidimensional environmental stimuli refine macrophage polarization and foster revolutionary approaches in tissue regeneration. Heliyon. 2024;10(17):e37192. doi:10.1016/j.heliyon.2024.e37192.
20. Li L, Yu F, Zheng L, Wang R, Yan W, Wang Z, et al. Natural hydrogels for cartilage regeneration: modification, preparation and application. J Orthop Translat. 2019;17:26–41. doi:10.1016/j.jot.2018.09.003.
21. Liu M, Zeng X, Ma C, Yi H, Ali Z, Mou X, et al. Injectable hydrogels for cartilage and bone tissue engineering. Bone Res. 2017;5(1):17014. doi:10.1038/boneres.2017.14.
22. Liu X, Hu Y, Ju Y, Yang P, Shen N, Yang A, et al. Immunomodulatory hydrogels for tissue repair and regeneration. APL Mater. 2024;12(8):080603. doi:10.1063/5.0228692.
23. Yang J, Lai M, Ma Y, Wu J, Zhang C, Yuan H, et al. Spatiotemporal modulation of immune microenvironment via composite hydrogel brakes for diabetic wound healing. Chem Eng J. 2024;493:152251. doi:10.1016/j.cej.2024.152251.
24. Wu Y, Gong Z, Li J, Meng Q, Fang W, Long X. The pilot study of fibrin with temporomandibular joint derived synovial stem cells in repairing TMJ disc perforation. Biomed Res Int. 2014;2014:454021. doi:10.1155/2014/454021.
25. Jang EJ, Patel R, Sankpal NV, Bouchard LS, Patel M. Alginate, hyaluronic acid, and chitosan-based 3D printing hydrogel for cartilage tissue regeneration. Eur Polym J. 2024;202:112651. doi:10.1016/j.eurpolymj.2023.112651.
26. Park KM, Lee SY, Joung YK, Na JS, Lee MC, Park KD. Thermosensitive chitosan-Pluronic hydrogel as an injectable cell delivery carrier for cartilage regeneration. Acta Biomater. 2009;5(6):1956–65. doi:10.1016/j.actbio.2009.01.040.

27. Sadeghianmaryan A, Naghieh S, Yazdanpanah Z, Alizadeh Sardroud H, Sharma NK, Wilson LD, et al. Fabrication of chitosan/alginate/hydroxyapatite hybrid scaffolds using 3D printing and impregnating techniques for potential cartilage regeneration. Int J Biol Macromol. 2022;204:62–75. doi:10.1016/j.ijbiomac.2022.01.201.
28. Fang Z, Liu G, Wang B, Meng H, Bahatibieke A, Li J, et al. An injectable self-healing alginate hydrogel with desirable mechanical and degradation properties for enhancing osteochondral regeneration. Carbohydr Polym. 2024;343:122424. doi:10.1016/j.carbpol.2024.122424.
29. Yang C, Chen R, Chen C, Yang F, Xiao H, Geng B, et al. Tissue engineering strategies hold promise for the repair of articular cartilage injury. Biomed Eng Online. 2024;23(1):92. doi:10.1186/s12938-024-01260-w.
30. Nie R, Zhang QY, Feng ZY, Huang K, Zou CY, Fan MH, et al. Hydrogel-based immunoregulation of macrophages for tissue repair and regeneration. Int J Biol Macromol. 2024;268:131643. doi:10.1016/j.ijbiomac.2024.131643.
31. Lai CM, Chen WJ, Qin Y, Xu D, Lai YK, He SH. Innovative hydrogel design: tailoring immunomodulation for optimal chronic wound recovery. Adv Sci. 2025;12(2):e2412360. doi:10.1002/advs.202412360.

Received: 04 June 2025; Accepted: 23 September 2025; Published: 31 December 2025